European Journal of Operational Research
Volume 259, Issue 3, 16 June 2017, Pages
1156-1168
https://doi.org/10.1016/j.ejor.2016.11.028

Stochastic short-term hydropower planning with inflow scenario trees

Sara Séguin[c,1,*], Stein-Erik Fleten[c], Pascal Côté[b,d], Alois Pichler[c], Charles Audet[a,b]

[a] *Department of Mathematics and Industrial Engineering, École Polytechnique de Montréal, C.P. 6079, succ. Centre-ville, Montréal, Québec, H3C 3A7, Canada*
[b] *GERAD, 3000 ch. de la Côte-Sainte-Catherine, Montréal, Québec, H3T 2A7, Canada*
[c] *Department of Industrial Economics and Technology Management, Norwegian University of Science and Technology, Trondheim, NO-7491, Norway*
[d] *Rio Tinto, 1954 Davis, Saguenay, Québec, G7S 4R7, Canada*

Abstract

This paper presents an optimization approach to solve the short-term hydropower unit commitment and loading problem with uncertain inflows. A scenario tree is built based on a forecasted fan of inflows, which in turn comes from the weather forecast and the historical weather realizations. The tree-building approach seeks to minimize the nested distance between the stochastic process of historical inflow data and the multistage stochastic process represented in the scenario tree. A two-phase multistage stochastic model is used to solve the problem. The proposed approach is tested on a 31 day rolling horizon with daily forecasted inflows for three power plants situated in the province of Quebec, Canada, that belong to the company Rio Tinto.

Keywords: Large scale optimization, nonlinear programming, OR in energy, scenarios, stochastic programming.

*Corresponding author
Email addresses: sara.seguin@gerad.ca (Sara Séguin), stein-erik.fleten@iot.ntnu.no (Stein-Erik Fleten), pascal.cote@riotinto.com (Pascal Côté), aloisp@ntnu.no (Alois Pichler), charles.aude@gerad.ca (Charles Audet)
[1] Permanent address: Department of Mathematics and Industrial Engineering, École Polytechnique de Montréal, C.P. 6079, succ. Centre-ville, Montréal, Québec, H3C 3A7, Canada and GERAD, 3000 ch. de la Côte-Sainte-Catherine, Montréal, Québec, H3T 2A7, Canada

1. Introduction

Hydroelectric producers invest time and resources in developing optimization tools to gain efficiency in the use of water, since these even small improvements lead to significant savings. Short-term optimization is used at the power plant level to dispatch available water for production between the turbines. Each turbine has a different efficiency. The amount of water available for production, or reservoir trajectories, is determined from the medium-term optimization and considers demand, uncertainty in the inflows and travel time of the water between the plants. Short-term optimization is often considered to be deterministic [1] by making the assumption that the inflows are known [2] or by neglecting water balance constraints [3] at such a short time scale, but does not allow planning under different forecasts. Also, [4] have shown that considering uncertainty in short-term decision models may lead to improvements.

The focus of this paper is stochastic optimization applied to the short-term hydropower optimization problem. By considering uncertain inflows, turbines will be used in a more efficient manner since the stochastic model results in a compromise between high and low forecasted inflows. For example, in situations where reservoirs are nearly full, considering uncertain inflows when important inflows are expected prevents lowering the reservoir and forcing turbines into inefficient zones, which results in energy production loss in the future if these high inflows do not occur.

Few papers have looked specifically into short-term hydropower models with uncertain inflows. In [5], a short-term hydropower optimization model treats deterministic inflows. Water head variations are considered and nonlinearities and nonconvexities of the hydropower production function are accounted for. In [6], uncertainty of prices and inflows is considered. They use time series analysis to model the water inflows, which is represented by a scenario tree in the stochastic programming model. Start-up costs are considered and a multistage stochastic model is approximated by a two-stage model. A mixed-integer linear program is used.

The net water head is assumed to vary with the water discharge only, so hydropower production functions depend only on the water discharge. In [7], the only uncertainty considered is demand. The deterministic model is a linear integer model, which is an approximation of a nonlinear mixed integer model. Once again, the hydropower production function depends only on water discharge. For some hydropower systems, neglecting the water head is not a possible avenue since many of the reservoirs have small capacities. Consequently, the water head effect is important in a short-term optimization, even with short time steps.

Many assumptions are made when solving the short-term unit commitment model, since they are complex to solve. They have a large amount of variables, power production functions are nonlinear and efficiency is different for every turbine. The most common assumption is to neglect water head variations leading to linear power production functions.

When uncertainty arises and one wants to solve optimization models, two main streams of ideas have been applied in the optimization community. Stochastic dynamic programming has been used extensively to solve hydropower optimization models [8, 9], as well as variants such as sampling stochastic dynamic programming [10] or stochastic dual dynamic programming [11]. These models are well suited for long or medium-term horizons but for short-term models, the state space is huge and it is very difficult, if not impossible, to solve them. In order to prevent the optimization process to empty out the reservoirs in the short-term model, values are assigned to the remaining water at the end of the planning horizon, which are obtained with stochastic dynamic programming or stochastic dual dynamic programming for example. In [12], a new method to generate inflows, based on periodic autoregressive models, is used as input to a stochastic dual dynamic programming algorithm that allows to schedule a hydro-thermal system located in Brazil.

The other stream is stochastic programming. A two-stage stochastic model [13] consists of two stages of decisions. The first stage decisions need to be taken without knowing the realization of the uncertainty in the future, while

the second stage decisions are taken when the uncertainty is revealed.

Usually, uncertainty is represented by scenarios. Each scenario is a possible realization of the uncertainty. Multiple scenario generation methods have been used in the past to approximate the distributions of the stochastic parameters. An overview of these methods, as well as evaluating the quality of a scenario tree is found in [14]. In [15], a periodic autoregressive process is used to fit historical data of the prices and to generate prices for the stochastic model. The scenario tree is built by sampling the distribution fitted with the model for the different nodes. Another method creates a discrete distribution of the uncertain parameter by matching some specific statistical properties. In [16], the first four moments, mean, variance, skewness and kurtosis are matched. Multiple pitfalls arise from this method and one must ensure the scenario tree represents possible outcomes of the uncertainty. A survey of techniques for generating scenario trees appears in [17] and includes recombining of data paths, contamination method and matching. More recently, copulas have been used to generate scenarios for two-stage stochastic problems [14]. This method offers the advantage of treating dependencies better than with correlation alone. Other methods are scenario reduction [18, 19]. An initial scenario tree is required and forward selection, or backward reduction is applied in order to reduce it and diminish computational time to solve the stochastic optimization model. The effect of the reduction on the solution accuracy, applied to a cascaded system of hydropower reservoirs is found in [20].

Other methods to deal with uncertainty on the inflows include robust optimization techniques [21] and probabilistic constrained programming [22]. Robust optimization solves models that have uncertain parameters over uncertainty sets. Therefore, the optimization seeks to find a solution that is feasible regardless of the outcome of the uncertainty. In [23], a rolling-horizon scheme is used and robust optimization is applied to the decision of day 1 while the rest of the horizon is considered deterministic. This is interesting as the uncertainty is applied to the important decisions. A drawback of robust optimization is the formulation of the uncertainty. In the historical records, some values of inflows

may be very low and others very high. Therefore, it is difficult to define what are the best bounds for the uncertainty set, as well as capturing any nonlinear dynamics present. In probabilistic constrained programming, constraints are to be respected given a certain probability. A cascaded hydropower reservoir is solved with probabilistic constrained programming in [22]. As with robust optimization, parameters on security-level and probability measures are to be given to the model, which is a difficult task in practice.

We contribute to the existing literature by considering inflow uncertainty in the short-term hydropower model. Few papers have looked specifically in stochastic short-term models and we extend the modeling proposed in [5] to consider uncertain inflows. For the producer, it is interesting to consider a stochastic model since it gives a production plan for the whole planning horizon. Applying the theory outlined in [24], we also detail/provide a nonparametric scenario generation approach that relies on the information in the history of inflows. We expand [5] by introducing stochasticity to both the loading and unit commitment problems.

The paper is organized as follows. Section 2 presents data available for inflows. Section 3 describes the method to generate scenario trees. Section 4 gives an overview of the short-term hydropower problem and details the optimization models. Numerical results are presented in Section 5 and final remarks are presented in Section 6.

2. Scenario fan of inflows

This section presents the data available for the inflows. In the province of Quebec in Canada, consumers and producers of hydroelectric energy, except Hydro-Quebec, are not allowed to bid on the spot markets [25]. The province-owned integrated utility performs all power market activities. Hence, only uncertainty related to inflows in the reservoirs is considered in this paper.

Before presenting the method for generating the scenario trees used in the optimization models, we pause to describe the available data sets. Precipitation

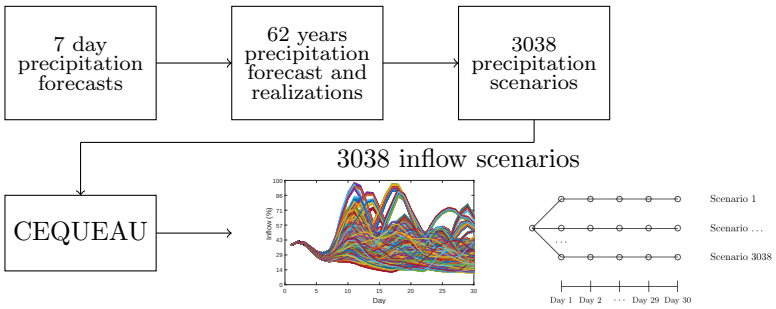

Figure 1: Building inflow scenarios from a 7 day deterministic precipitation forecast.

forecasts are obtained from Environment Canada [26]. A 7 day deterministic precipitation forecast is issued. The 7 day forecast is split in two groups: the first 3 and the last 4 days. We make the assumption that the error for both groups is independent from a meteorological point of view, as the correlation in precipitations between days is negligible. This assumption is motivated by the great variability in Canadian weather conditions from one day to the next. For example, we could have a few days of snow, followed by no precipitations then a few days of rain. The last 15 years of historical data of precipitation forecasts is searched for a given number (a) of precipitation forecasts that are the closest, in precipitation forecast (mm) to the first 3 days, and they are retained. The same is conducted for the second group. Since the error is assumed independent, the scenarios found for the first and second group are mixed and matched to create a^2 precipitation scenarios for the first 7 days. Note that the actual realizations of precipitation on these days are used as scenarios. Then, considering that the forecast has no value after 7 days, the 62 years of available history of realizations is appended to all of the scenarios for the first 7 days with $a = 7$, yielding a total of $a^2 \times 62 = 3038$ scenarios of precipitation for 30 days of prevision. Then, these precipitation scenarios are given as input to the CEQUEAU hydrological model [27] which outputs inflow previsions for the reservoirs.

Figure 1 illustrates this process. The goal of the scenario tree generation method, in Section 3, is to create a scenario tree from the scenario fan of inflows.

3. Scenario tree generation

The method chosen to construct a scenario tree suitable for the stochastic optimization is taken from [24, 28]. The method is applied to real hydropower data. First, the structure of the scenario tree is fixed, then stochastic approximation is used to improve the states of the nodes, considering all the data available for every approximation. Improvement goes on until a convergence criteria, based on the nested distance and explained in Section 3.4, is reached.

3.1. Fixing the initial scenario tree structure: k-means clustering

The stage and the number of nodes per stage of the tree is fixed initially, more precisely, the number of stages as well as the number of nodes per stage. Aggregation is necessary since the scenario tree structure can be different from the data available. The aggregation is straightforward: values of inflows for each day are summed up.

K-means clustering [29] is used to partition the data paths into clusters in order to assign initial values to the scenario tree nodes. Note that initially no probabilities are allocated to the nodes: simply values for the nodes. This clustering method minimizes the distance from every data point to the mean of the cluster to which it belongs. As an example, the k-means algorithm is applied to the 3038 inflow scenarios to form a scenario tree which has a structure as per Figure 3b.

3.2. Improvement of the clusters

The method to improve the scenario tree nodes consists of two steps. First, from the initial data paths, a random data path, that is not in the paths available, is generated using density estimation. Next, the distance between this random path and the closest state of the scenario tree nodes is minimized in a stochastic approximation step in order to improve the tree. This method is repeated for a given number of iterations and is explained in what follows.

3.2.1. Step I: density estimation

In order to generate a new random path, kernel density estimation is used. We generate a random path that is close to the distribution of the data paths and conditional on previous stages. To do so, the conditional probability density function is estimated. For each stage of the desired scenario tree structure a value of inflow is generated that is close in distribution to all of the data paths and incidental to the past.

A random path $\xi_k^d = (\xi_1^d, \ldots, \xi_K^d)^T$ is to be generated using available data paths $X_{ik}^d = (X_{i1}^d, \ldots, X_{iK}^d)^T$ where i is the index of available data paths, d is the dimension and K is the number of stages. The conditional density estimator is:

$$\hat{f}\left(\xi_k|\xi_1, \ldots, \xi_{k-1}\right) = \sum_{i=1}^{n} \prod_{j=1}^{k-1} \frac{\kappa\left(\frac{\xi_j - X_{ij}}{h_j}\right)}{\sum_{m=1}^{n} \kappa\left(\frac{\xi_j - X_{mj}}{h_j}\right)} \times \kappa\left(\frac{\xi_k - X_{ik}}{h_k}\right) \times \frac{1}{h_k}, \quad (1)$$

where the dimension d is dropped for clarity, n is the number of available data paths, κ is the kernel and h is the bandwidth.

The analytical representation of the actual distribution is not computed, as only samples from Equation (1) are necessary which can be generated quickly. In practice, this is achieved by assigning weights to every data path available. The closer the observation is to the path, the higher is the weight. For every stage from $1, \ldots, k-1$, the weights of the data path at each stage are multiplied. With these weights calculated, a value of inflow is to be generated at stage k.

To illustrate refer to Figure 2. There are three data paths of inflow. The random value of inflow has been generated for stage 1 and is located with a star marker. From there, a value of inflow is to be generated for subsequent stages, always conditional on the past. As per the figure, it is necessary to find a value of inflow at stage 2 that is consistent with the conditional distribution. Therefore, weights are calculated as follows, in this case for stage k:

$$w_i(\xi_1, \ldots, \xi_{k-1}) = \prod_{j=1}^{k-1} \frac{\kappa\left(\frac{\xi_j - X_{ij}}{h_j}\right)}{\sum_{m=1}^{n} \kappa\left(\frac{\xi_j - X_{mj}}{h_j}\right)}, \quad (2)$$

where $\sum_{i=1}^{n} w_i = 1$ and $w \geq 0$.

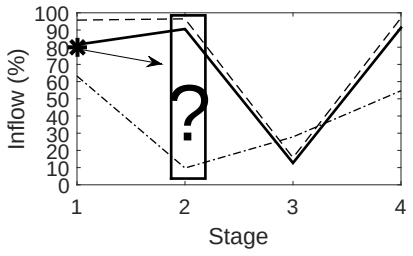

Figure 2: Generation of a random path based on three available data paths of inflows. The generated value of inflow for stage 1 is shown with a star marker.

The value of inflow ξ_k at stage k is generated as follows. A data path with index i^* is chosen randomly among the available data paths at stage $k-1$ to satisfy

$$\sum_{i=1}^{i^*-1} w_i(\xi_1, \ldots, \xi_{k-1}) \leq \text{rand}_u \leq \sum_{i=1}^{i^*} w_i(\xi_1, \ldots, \xi_{k-1}), \tag{3}$$

where rand_u is chosen from the uniform random distribution on the interval $[0, 1]$. The cumulative sum of the weights leads to a high probability of picking a data path near an observation.

The value of inflow ξ_k is obtained by setting the value at stage k

$$\xi_k = X_{i^*k} + \text{rand}_{\kappa_{h_k}}, \tag{4}$$

where $\text{rand}_{\kappa_{h_k}}$ is a random value sampled from the kernel estimator using the composition method [24].

This newly generated inflow value is according to the distribution of density of the current stage and dependent on the history of all the data paths.

Referring again to Figure 2, weights are calculated for the 3 data paths as per Equation (2). Then, a data path is chosen randomly at stage 1 and the thick filled line has a high probability of being picked. Consider it is the case. To generate the value of inflow at stage 2, the value of the thick filled line at stage 2 is perturbed randomly. This method is then repeated at each stage in order to generate a random data path and is represented on Figure 3a with a

thick dashed line.

It is shown that the choice of the kernel does not have an important effect on the density estimation [30]. Hence, in this paper, the logistic kernel is used:

$$\kappa(\xi) = \frac{1}{e^{\xi} + 2 + e^{-\xi}}. \tag{5}$$

The bandwidth is the smoothing factor applied to the estimation of the density. Silverman's rule of thumb [31] is employed to determine the optimal bandwidth:

$$h_k = \sigma(X_{ik}) n^{-\frac{1}{d+4}} = \sigma(X_{ik}) n^{-\frac{1}{7}}, \tag{6}$$

where n is the number of data paths, d is the dimension and σ is the standard deviation. In this paper, $d = 3$ because there are three values of inflows per scenario tree node, representing three different reservoirs.

3.2.2. Step II: stochastic approximation

Once the new random path of inflows is generated, a stochastic approximation step is conducted. This step allows to update the value of some scenario tree states. During this step, a scenario from the scenario tree, more precisely a path of nodes in the scenario tree is identified. This path of nodes in the scenario tree minimizes the Wasserstein distance W between the random generated path during Step I of the algorithm, found in Section 3.2.1, and current scenario tree nodes values.

The Wasserstein distance is minimized as follows:

$$W^2 = \min_{\omega \in \Omega} \sum_{k=1}^{K} ||\Gamma(\omega) - \xi_k||^2, \tag{7}$$

where Ω are the scenario tree paths, $\Gamma(\omega)$ are the states corresponding to the nodes in the path ω in the scenario tree, from the set of all possible scenarios Ω, and ξ_k is the value of inflow generated randomly at stage k. Referring to Figure 3b, $\Omega = \{(1,2,3,5),(1,2,3,6),(1,2,4,7),(1,2,4,8)\}$. Equation (7) allows to find this path of nodes and is identified as $\omega = (1,2,4,8)$ on Figure 3b.

To achieve this, a stochastic gradient descend method that minimizes the nested distance is used. Starting from the root of the scenario tree, W is com-

puted for the children node. The children node with the smallest value of W becomes the parent node. W is then computed for the children node of the new parent node and so on until a leaf node has been reached.

The identified path of scenario tree nodes values $\Gamma(\omega)$ that minimizes the Wasserstein distance for the current stochastic approximation iteration $p = 1, 2, \ldots$ is updated in the following manner:

$$\Gamma(\omega)_{p+1} = \Gamma(\omega)_p - \alpha_p \nabla W_p, \tag{8}$$

where $\Gamma(w)$ are the values of the scenario tree nodes to improve, α_p is the step-size and ∇W_p the gradient of the distance.

The step-size $\alpha_p = \frac{1}{(p+30)^{3/4}}$, where p is the stochastic approximation iteration, is chosen since it is shown that the method will converge since $\alpha_p > 0$, $\sum_p \alpha_p = \infty$ and $\sum_p (\alpha_p)^2 < \infty$.

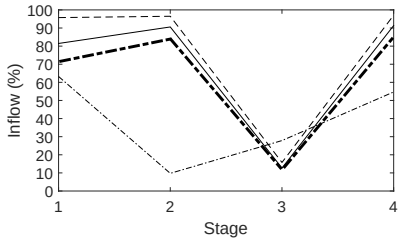

(a) Randomly generated path of inflows, shown with thick dashed line, from three available data paths of inflows.

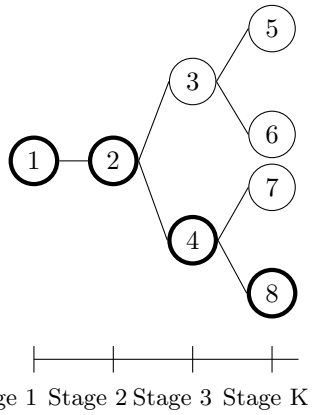

(b) Scenario tree. The path of nodes in the scenario tree that minimizes the Wasserstein distance is shown in bold.

Figure 3: Illustration of the 2 steps of the algorithm. Generation of a random path of inflows from available data paths of inflows and stochastic approximation to improve the value of some scenario tree nodes.

As an illustration, consider one iteration of the algorithm and refer to Figure 3. First, a random data path of inflows is generated using kernel density estimation. This can be seen on Figure 3a: it is the thick dashed line. The Wasserstein

distance between this new generated path of inflows and the current values of the scenario tree nodes is minimized and a path of nodes in the scenario tree is retrieved in order to be improved. The path of nodes minimizing this distance is shown on Figure 3b. Hence, the value of the inflows for the thick nodes, which are 1, 2, 4 and 8 will be improved using Equation (8).

3.3. Probabilities

During the first stochastic approximation iteration, assigned probabilities of the nodes are 0 since, as explained in Section 3.1, the scenario tree is initialized with values for the nodes only.

Node probabilities are updated every stochastic approximation iteration. A counter is assigned to each node and initialized at 0. Every time a path of nodes minimizing the Wasserstein distance is retrieved, the corresponding counters of the nodes in this path are incremented by 1.

Once the stochastic approximation iterations are completed, probabilities are computed by dividing the counter value with the number of stochastic approximation iterations, which yields sums of child nodes probabilities equal to 1, as in Figure 4.

In a multistage stochastic program model, each path from the root to a leaf node represents a scenario. The unconditional probabilities of a scenario is obtained by multiplying the unconditional probabilities of all the nodes in the scenario, yielding probabilities π_j, where j is the scenario in Figure 4.

An interesting feature of the scenario tree generation method is that the extreme (low and high) scenarios are accounted for, according their occurrence in the historical data set. The law of large numbers insures that the probabilities are asymptotically consistent.

3.4. Termination criterion

The scenario tree generation algorithm terminates when the nested distance has converged to a certain ϵ for the 10 last iterations. Thus, Step I and Step II of the algorithm are repeated until convergence is obtained.

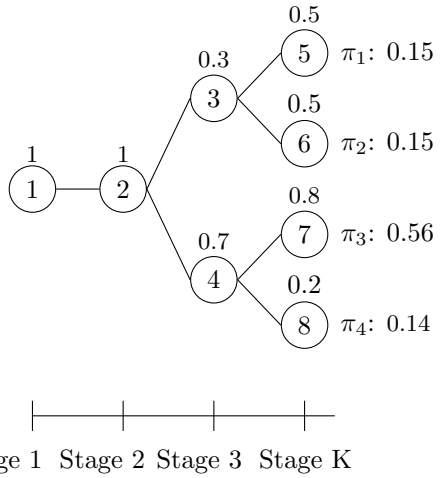

Figure 4: A scenario tree with node probabilities (over the node) and scenario i probabilities (indicated with π_i)

The main advantage of the scenario tree generation method presented in this section is that all of the data paths are used at every iteration to improve the value of the scenario tree nodes. By doing so, the underlying discrete distribution of the available data paths, approximated by a scenario tree, is improved consistently with the data.

4. Stochastic short-term hydropower model

The two phase deterministic optimization models taken from [5] are updated to consider stochastic inflows. This section presents the modeling of the short-term problem as well as the mathematical formulations.

4.1. Modeling of the short-term problem

The modeling of the problem considers head-dependency, as well as efficiencies of each turbine. Power $P(kW)$ produced by a single turbine is defined as

$$P(h_n, Q) = \eta(Q) \times G \times Q \times h_n(Q_{tot}, v), \tag{9}$$

where G is the gravitational acceleration (m/s^2), Q is the unit water flow and Q_{tot} is the total water flow (m^3/s), $\eta(Q)$ is the efficiency of the turbine and h_n is the net water-head (m). The net water-head is a function of the forebay elevation h_f (m), the tailrace elevation h_t (m) and losses in the penstock φ (m) that is given by:

$$h_n(Q_{tot}, v) = h_f(v) - h_t(Q_{tot}) - \varphi(Q_{tot}), \tag{10}$$

where v is the volume of the reservoir (hm^3). For notational purposes and since there is a relation between net water head and volume, we consider that power is a function of the volume and water flow. We propose a modeling with combinations of units instead of single units. To achieve this, a dynamic programming algorithm, where each sub-problem is a turbine, is used to calculate the power produced by a combination of units. As an example, if a power plant has a total of 5 turbines and requires three active turbines, there is a total of 10 combinations of 3 turbines, 5 combinations of 4 turbines and 1 combination of 5 turbines. Water flows are discretized and the dynamic programming algorithm is executed for each possible combinations, 16 in this case, for each power plant and discretizations of reservoir volumes and water flows.

4.1.1. Dynamic programming algorithm

The objective of the problem is to maximize the power output and it is found recursively. Given state s^j, the dynamic programming algorithm seeks to choose decision variables q^j that solves:

$$f^{*j}(s^j) = \max_{q^j} P(s^j, v) + f^{*j+1}(s^j - q^j), \tag{11}$$

where $j = n-1, n-2, \ldots, 1$, n is the number of turbines at the power plant, $s^j \in \{1, 2, \ldots, r\}$ is the remaining water to dispatch given the number of discretizations r and $q^j \in \{1, 2, \ldots, \min\{\overline{q^j}, Q\}\}$ the water flow with $\overline{q^j}$ maximum water flow. The optimal water flow is $q^{*j} = s^j$ that maximizes $f^{*j}(s^j)$. For $j = n$, the optimal power output is given by $f^{*j}(s^j) = P(s^j)$.

4.1.2. Maximum power output surfaces

We then build one surface of the maximum power output for each power plant. For a plant with 5 turbines requiring at least 3 working, three surfaces are built, more precisely one for 3 turbines working, one for 4 turbines working and one for 5 turbines working. The maximum power output for every possible combination of number of working turbines is retained for every discretization of volume and water flow. Such surfaces can be viewed in Figure 5. To ob-

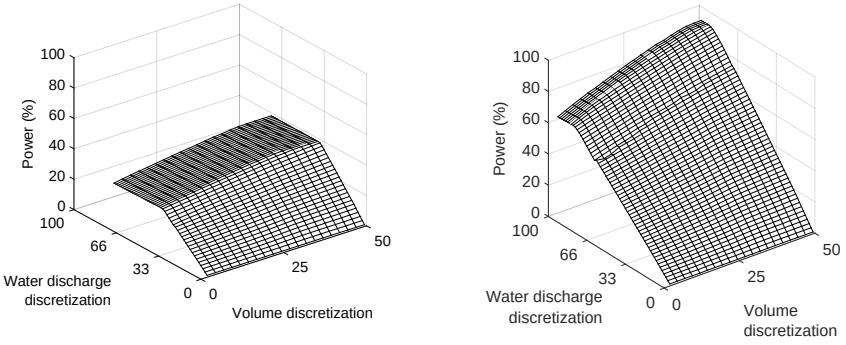

(a) Five turbines in the combination

(b) Twelve turbines in the combination

Figure 5: Maximum output surfaces

tain them, the dynamic programming algorithm is executed for every number of turbines in the combination, every discretization of the reservoir volume, every discretization of the water flow and every power plant. The surfaces of maximum power outputs are then modeled using polynomial equations in the objective-function of the optimization problem. Modeling of the hydropower production functions is done by constraining these functions with two surfaces. A two-phase optimization strategy is used to penalize the startup of turbines. The first phase, namely the loading problem, optimizes values of water discharges, volumes and number of turbines in the combination for every plant and node. The second phase, namely the unit commitment problem, uses the solution of the first optimization model to determine the exact combination of turbines working at each plant and node in the scenario tree. Startups of

turbines are penalized with a fixed cost. Multistage stochastic models are developed for both optimization phases, in order to consider uncertainty in the inflows of the reservoirs.

4.2. Phase I: loading problem

Optimization variables of this nonlinear stochastic multistage mixed integer problem are water flows, volumes and number of working turbines, for each node and plant in the scenario tree. The model must choose one surface of number of working turbines among those available, but we have shown [5] that relaxing these variables leads to an integer solution. Therefore, we solve a nonlinear stochastic multistage continuous problem.

The objective is to maximize total energy production in stage 0, expected energy production in future stages and expected value of the water remaining in the reservoir at the end of the planning horizon:

$$\max \quad \sum_{c\in C}\sum_{s=1}^{n_0^c} \chi_{s0}^c y_{s0}^c \zeta_0 + \sum_{j\in J}\sum_{c\in C} \pi_j^c P_j^c + \sum_{c\in C}\sum_{j\in E} \pi_j^c \Phi_j^c(V_j^c) \tag{12}$$

$$\text{subject to:} \quad \chi_{si}^c \le \Psi_s^{Ac}(q_i^c, v_i^c), \qquad \forall c \in C, \forall i \in N, \forall s \in n_i^c \tag{13}$$

$$\chi_{si}^c \le \Psi_s^{Bc}(q_i^c, v_i^c), \qquad \forall c \in C, \forall i \in N, \forall s \in n_i^c \tag{14}$$

$$\delta_i^c = v_{i+1}^c - v_i^c + \gamma w_i q_i^c - \sum_{m=1}^{u^c} \gamma w_m q_m, \qquad \forall i \in N, \forall c \in C \tag{15}$$

$$\sum_{s=1}^{n_i^c} y_{si}^c \le 1, \qquad \forall i \in N \tag{16}$$

$$y_{s0}^c = \hat{y}_{s0}^c, \qquad \forall s \in n_i^c, \forall c \in C, \forall i \in N \tag{17}$$

$$v_{min}^c \le v_i^c \le v_{max}^c, \qquad \forall i \in N, \forall c \in C \tag{18}$$

$$q_{min}^c \le q_i^c \le q_{max}^c, \qquad \forall i \in N, \forall c \in C \tag{19}$$

$$q_i^c \ge 0, \forall i \in N, \qquad \forall c \in C \tag{20}$$

$$v_i^c \ge 0, \forall i \in N, \qquad \forall c \in C \tag{21}$$

$$y_{si}^c \ge 0, \qquad \forall s \in n_i^c, \forall i \in N, \forall c \in C. \tag{22}$$

Hydropower production surfaces are constrained by (13)-(14). Water balance constraints are represented by (15) and the choice of a single number of active turbines is shown in (16). Constraints (17) are the initial number of active turbines while constraints (18)-(19) are the bounds on reservoir volumes and water discharges. Finally, constraints (20)-(22) impose nonnegativity.

The above short-term loading problem is described in more details in [5]. We now show how to integrate a water-value function for the remaining water at the end of the planning horizon.

Water-value function. The water-value function is the expected energy production in the future at the end of the planning horizon. In a deterministic framework, inflows are known with certainty, thus volume in the reservoir at the end of the horizon is easier to determine. In a stochastic framework, it is not possible to give a goal for the volume at the end of the horizon since it may not be feasible for every scenario. On the other hand, neglecting this feature will cause the optimization to empty the reservoir at the end of the horizon, since the objective is to maximize energy. Hence, maximizing the expected value of future energy production, or water-value function, will prevent the optimization of doing this. The water-value functions are computed with a stochastic dynamic algorithm [32] at Rio Tinto. A planning horizon of one year, with weekly time steps is used.

4.3. Phase II: unit commitment

This linear stochastic multistage integer model is solved using solution found in Phase I. The purpose of this model is to determine the on-off schedule of the turbine combinations (found in Phase I). Given water flows and reservoir volumes found in the loading problem, the dynamic programming algorithm is used to calculate power outputs for every possible combination of turbines, given the number of working turbines found in Phase I, and are stored in parameter β_{li}^{c}. The model maximizes the energy production and penalizes turbine startups. Initial combination of turbines working at stage 0 is given in $\hat{x}_{l0}^{c}$.

The objective is to maximize energy production at stage 0 and future energy production and penalize startup of turbines at stage 0 as well as future expected startups:

$$\max \quad \sum_{c\in C}\sum_{l=1}^{n_0^c} \beta_{l0}^c x_{l0}^c \zeta_0 - \sum_{c\in C}\sum_{t=1}^{T^c} d_{t0}^c \theta \zeta_0 + \sum_{j\in J}\sum_{c\in C} \pi_j^c E_j^c - \sum_{j\in J}\sum_{c\in C} \pi_j^c G_j^c \quad (23)$$

$$\text{subject to:} \quad \sum_{l=1}^{n_i^c} x_{li}^c = 1, \qquad \forall i \in N, \forall c \in C \quad (24)$$

$$x_{li}^c f_{lit}^c - x_{li-1}^c f_{li-1t}^c \leq d_{ti}^c, \qquad \forall l \in n_i^c, \forall i \in N, \forall c \in C, \forall t \in T^c \quad (25)$$

$$x_{l0}^c = \hat{x}_{l0}^c, \qquad \forall l \in n_i^c, \forall i \in N, \forall c \in C \quad (26)$$

$$x_{li}^c, d_{it}^c \in \mathbb{B}, \qquad \forall l \in n_i^c, \forall i \in N, \forall t \in T^c, \forall c \in C. \quad (27)$$

The choice of a single turbine combination is given by (24). Constraints that allow to penalize a startup by flagging them is shown in constraints (25). The initial combinations are given in (26) and imposition of binary variables are constraints (27).

This two phase optimization process allows to find a solution efficiently. Also, even though an approximation of the energy produced is conducted in the first phase, the actual energy production is retrieved in the second phase, seeing that the actual hydropower production functions are used to compute the actual energy production given a water discharge and volume, which are solutions of the first phase.

5. Results

This section details the system on which the stochastic hydropower models are tested and results are presented.

5.1. Hydroelectric system studied

The hydroelectric system studied is situated in the Saguenay Lac-St-Jean region in the province of Quebec, Canada and is owned by Rio Tinto. For the purpose of this paper, three hydroelectric plants, which are Chute-du-Diable,

Chute-Savane and Isle-Maligne are considered. The two first plants have 5 turbines each and the latter has 12. Figure 6 represents the system studied. Triangles represent reservoirs and squares power plants.

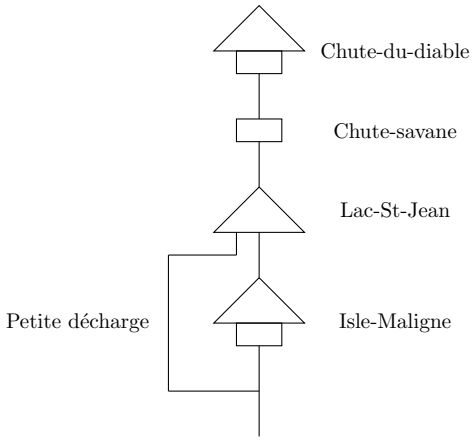

Figure 6: Hydroelectric system studied.

Chute-du-Diable, Chute-Savane and Isle-Maligne plants reservoir are quite small, respectively 452 hm^3, 119 hm^3 and 171 hm^3. In the optimization model, there is no water value function associated to these plants since they have small reservoirs. Instead, a full reservoir constraint at the last period is imposed as a goal in the model. The only water-value function used is for the Lac-St-Jean reservoir, therefore volume of this reservoir at the last period is an optimization variable. The capacity of this reservoir is of 5596 hm^3. Water flow in *Petite décharge* is limited by a function dependent on the volume of Lac-St-Jean.

5.2. Rolling horizon procedure

A rolling horizon methodology is retained to validate the optimization models developed in this paper. The planning horizon of the rolling-horizon is of 31 days. For every day of the rolling-horizon, the forecast is for 30 days. For day 1 of the rolling-horizon, previsions are from days 2 to 31, for day 2 of the rolling-horizon, previsions are from days 3 to 32, and so on. The stochastic optimization models presented in section 4 are solved every day, but only the

solution for the first stage is retained. Forecasts are updated daily. Once the forecast is updated, the scenario tree is generated for the corresponding day. The two-phase optimization process is launched and the first stage solution is retained, that is: volume, water discharge and turbine combination. Then, considering the actual realization of the inflow, the water balance constraints are used to determine the actual volume of the reservoirs at the end of the period. More precisely, the water discharge from the optimization is combined with the actual realization of the inflow in order to calculate the reservoir volumes. The same process is repeated for the 31 days. In the end, a production plan for 31 days is available, which consists of the reservoir volumes, total water discharges at the plants and turbine combinations in use. See [33] for a different approach to rolling-horizon evaluation of short-term hydropower operation.

The solution obtained from the scenario tree generation is compared to the solution obtained from the median scenario of the inflows. Therefore, we compare our method to a rolling median. Every day, the median scenario is found throughout all available scenarios and a scenario tree of 1 node per stage is solved in a deterministic fashion.

5.3. Numerical results

The scenario tree generation method is coded in Matlab [34]. The optimization models are coded through AMPL [35]. The optimization software for the loading problem, which is the relaxation of a nonlinear mixed-integer problem, is IPOPT [36] and the unit commitment model, a linear integer problem, is solved with XPRESS [37].

Six test cases, which consist of monthly periods are available. The biggest problems to solve have 7 stages with 48 scenarios, 1123 nonlinear variables, 33 linear variables and 1237 constraints for the loading problem and 3475 binary variables and 825 constraints for the unit commitment problem.

Different stages, more precisely 5, 6 or 7 as well as different number of scenarios, namely 16, 32 or 48 are tested.

5.3.1. Computational time

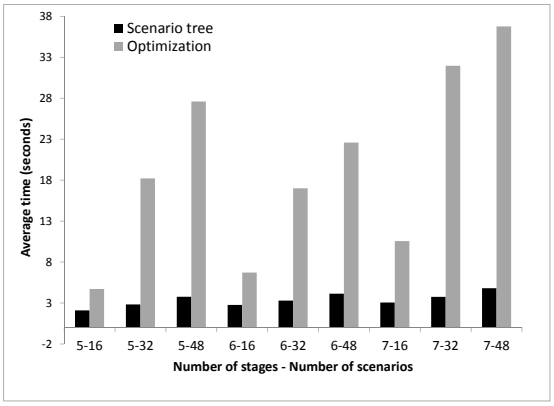

Figure 7: Average computational time of scenario tree generation and optimization for one day in the rolling-horizon.

The average time to construct the scenario tree and to optimize is shown on Figure 7. The average time is in seconds, for a single day in the rolling horizon procedure, more precisely for one problem including construction of the scenario tree and optimization of the two phase process. It takes less than 5 seconds to build the scenario trees for all test cases, while the optimization requires more time given higher numbers of scenarios. Less than 42 seconds, for a single day in the rolling-horizon are necessary to construct the scenario tree and optimize the two-phase process, which is acceptable in the real operating environment. The current implementation of the scenario tree generation method and optimization is tested on three cascaded hydropower plants. For this specific producer, the whole hydropower systems consists of five hydropower plants, therefore calculation time would be acceptable for the whole system. Considering another system of, for example, 50 hydropower plants, the actual method would take approximately 350 minutes. The proposed method in this paper is applicable to a larger system, probably by decomposing the system in smaller sub-systems. To do so, the system is to be studied and depending on its configuration, distances

between plants and others, modeled in an acceptable manner. Depending on the scope of the application, the calculation time may or may not be satisfactory. If a producer does not mind solving a 7 hour model every day, then the computational time is satisfactory. In order to diminish computing time, an avenue is to solve the model for a given number of days then weeks. In this way, the number of variables is greatly reduced and so is the computing time. This model is applicable to a larger hydropower system, but it would be necessary to decompose the system in sub-systems and review the modeling to diminish the number of optimization variables, given a producer requiring fast computational time.

5.3.2. Results

Table 1 illustrates the difference in energy, in TWh, produced throughout the 31 days rolling horizon combined with the value of water remaining in the reservoir at the end of the planning horizon. This implies that the difference in energy can be compared to annual production but absolute numbers are unfortunately not thus interpretable. A positive value indicates the scenario tree method produces more than the median scenario and a negative value indicates the contrary. For 4 of the test cases, the stochastic solution produces more energy. For 1 test case, the median scenario solution produces more energy. Finally, for the August case, the stochastic solution produces more energy with a 5 stage or 6 stage scenario tree, and the median scenario with a 7 stage. For the 4 test cases for which the scenario tree produces more energy than the median scenario, average improvements are 0.0679812% for June, 0.0273551% for July, 0.1620522% for September 2011 and 0.0251653% for September 2010. Despite the low percentages, this represents huge savings for the producer. As an example, the current value of a 1 GWh improvement, in the province of Quebec, is around 20,000$. Therefore, for June, the 0.0679812% higher production translates into 10,932,489$.

	June 2011			**July 2011**			**August 2011**		
Nb. Sc.	Stoch. (TWh)	Median (TWh)	Diff. (TWh)	Stoch. (TWh)	Median (TWh)	Diff. (TWh)	Stoch. (TWh)	Median (TWh)	Diff. (TWh)
	5 stages								
16	804.5143	804.0265	0.4878	740.2678	740.0631	0.2047	710.1115	710.0795	0.0320
32	804.7050	804.0251	0.6799	740.2783	740.0631	0.2152	710.1108	710.0794	0.0314
48	804.6894	804.0249	0.6645	740.2496	740.0631	0.1865	710.0988	710.0794	0.0194
	6 stages								
16	804.5059	804.1495	0.3564	740.2698	740.0665	0.2033	710.0783	710.0733	0.0050
32	804.6796	804.1479	0.5317	740.2652	740.0665	0.1987	710.1139	710.0733	0.0406
48	804.6715	804.1481	0.5234	740.2608	740.0665	0.1943	709.9826	710.0732	**-0.0906**
	7 stages								
16	804.5171	804.0881	0.4290	740.2676	740.0578	0.2098	710.0693	710.0867	**-0.0174**
32	804.7166	804.0881	0.6285	740.2566	740.0578	0.1988	710.0732	710.0867	**-0.0135**
48	804.7063	804.0879	0.6184	740.2686	740.0578	0.2108	710.0806	710.0867	**-0.0061**
	September 2010			**September 2011**			**October 2011**		
Nb. Sc.	Stoch. (TWh)	Median (TWh)	Diff. (TWh)	Stoch. (TWh)	Median (TWh)	Diff. (TWh)	Stoch. (TWh)	Median (TWh)	Diff. (TWh)
	5 stages								
16	729.5792	729.3811	0.1981	733.0375	731.6799	1.3576	704.7842	704.8494	**-0.0652**
32	729.5841	729.3821	0.2020	733.0530	731.6799	1.3731	704.7847	704.8494	**-0.0647**
48	729.5810	729.3804	0.2006	733.0818	731.6799	1.4019	704.7877	704.8496	**-0.0619**
	6 stages								
16	729.5856	729.3917	0.1939	732.9971	731.7773	1.2198	704.7690	704.8636	**-0.0946**
32	729.5779	729.3929	0.1850	733.0188	731.7773	1.2415	704.7928	704.8636	**-0.0708**
48	729.5800	729.3924	0.1876	733.0937	731.7774	1.3163	704.7326	704.8634	**-0.1308**
	7 stages								
16	729.5854	729.4151	0.1703	732.9428	731.9647	0.9781	704.7608	704.8566	**-0.0958**
32	729.5775	729.4156	0.1619	732.9599	731.9647	0.9952	704.7879	704.8566	**-0.0687**
48	729.5834	729.4139	0.1695	732.9702	731.9648	1.0054	704.7873	704.8567	**-0.0694**

Table 1: Results for 6 test cases (5 are data sets from the year 2011 and 1 from 2010). Energy produced by the stochastic solution and the median scenario rolling horizon is given. Also, the difference in energy between both solutions is shown.

5.3.3. In sample stability test

An in sample stability test allows to verify if the scenario tree generation method is consistent. It is taken from [38]. Since the scenario tree is generated from random samples, one wants to verify if the solution given by the optimization, with a different scenario tree each time, give more or less the same solution. If so, then the scenario tree method is consistent.

As an example, July 2011 and June 2011 data sets were chosen for this verification. For both data sets, 6 scenario trees were generated with the same number of stages and scenarios. Then, the optimization was conducted on all of these scenario trees to verify the effect on the objective function value. Table 2 gives, for these two data sets and 6 instances each, the values of the objective function, for the scenario tree and median scenario methods.

Data	Inst.	Stoch. (TWh)	Median (TWh)	Diff. (TWh)
July	1	740.2652	740.0665	0.1987
	2	740.2759	740.0665	0.2094
	3	740.2725	740.0665	0.2060
	4	740.2581	740.0665	0.1916
	5	740.2799	740.0665	0.2134
	6	740.2878	740.0665	0.2213
June	1	804.6715	804.1481	0.5234
	2	804.6707	804.1484	0.5223
	3	804.6709	804.1474	0.5235
	4	804.6824	804.1489	0.5335
	5	804.6769	804.1486	0.5283
	6	804.6571	804.1472	0.5099

Table 2: Objective function values for 6 random scenario trees with the same number of stages and scenarios, on two data sets.

Results show that the scenario tree generation method is consistent, as the

difference between the objective functions of the stochastic and median scenario methods present slight variations. For the July test case, the median is 0.2077 TWh, the mean 0.2067 TWh and the variance 0.9308 TWh and for the June test case, the median and the mean are 0.5235 TWh and the variance 0.0516 TWh.

5.3.4. Interpretation of the results

The following figures illustrate the 31 day rolling horizon backtesting solution more precisely: water discharge and reservoir levels for the power plants and reservoirs studied in this paper.

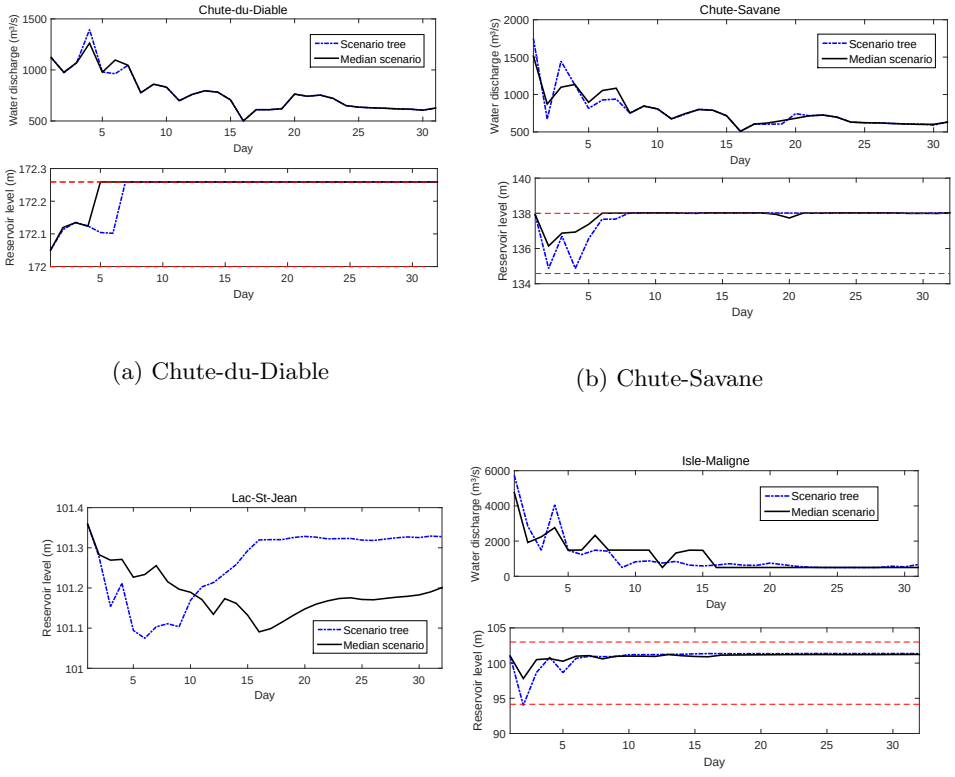

(a) Chute-du-Diable

(b) Chute-Savane

(c) Lac-St-Jean

(d) Isle-Maligne

Figure 8: June 2011, 5 stages, 16 scenarios.

Figure 8 pictures June 2011 data set with 5 stages and 16 scenarios. Solutions obtained from the scenario tree method and the median scenario are quite similar. Also note that when a method turbines more water, it is penalized accordingly so it is not advantaged. The difference between the volumes at the end of the 31 day planning horizon is taken into account and transformed into energy, then added to the method that is disadvantaged.

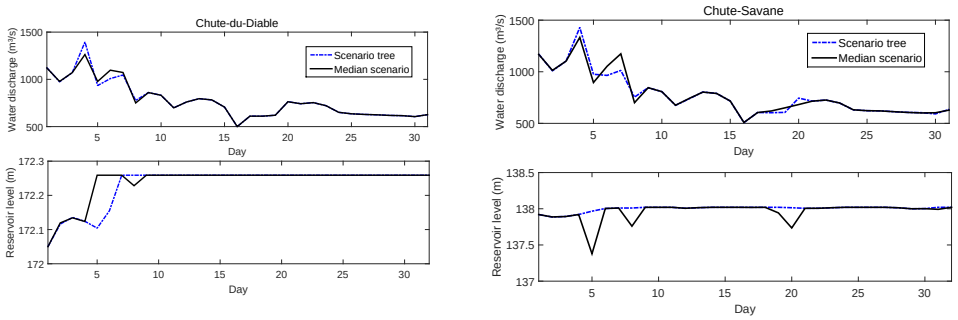

(a) Chute-du-Diable

(b) Chute-Savane

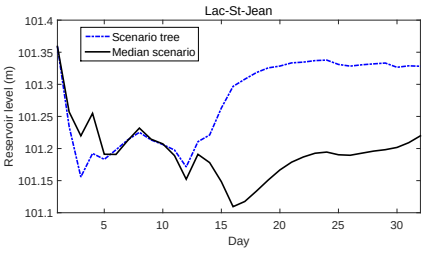

(c) Lac-St-Jean

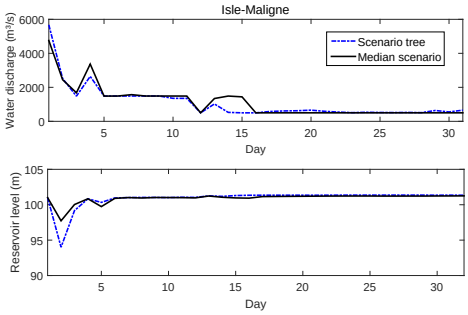

(d) Isle-Maligne

Figure 9: June 2011, 7 stages, 16 scenarios.

Figure 9 also illustrates the June 2011 data set with 7 stages and 16 scenarios. Again, results are very similar.

Without any surprise, the numerical experiment reveal that the solutions to the cases with more stages are closer to the operational ones because the hydropower sytem operation is more realistic. For example, Figures 8 and 9

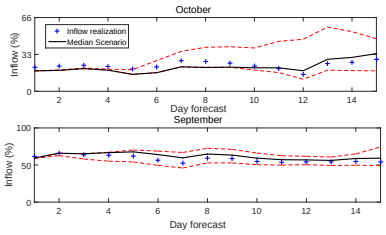

(a) Chute-du-Diable

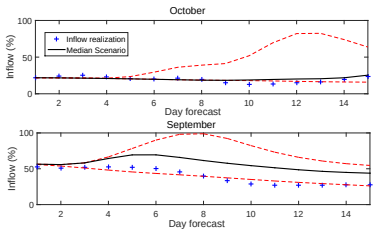

(b) Chute-Savane

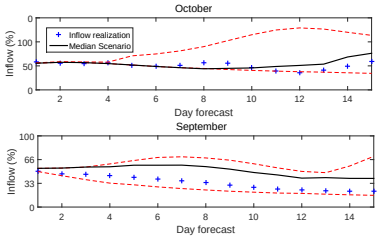

(c) Lac-St-Jean

Figure 10: Comparison of September (upper figures in each subfigure) and October (lower figures in each subfigure) day 1 data sets. The dashed lines are the minimum and maximum scenarios. The median scenario is the full line. The actual realization of the inflows is the plus sign line.

show that the solutions with 5 and 7 stages lead to a similar improvement, but the implementation with 7 stages is preferable. Figures 9a, 9b and 9d present reservoir volumes that are more stable than Figure 8a, 8b and 8d.

The October data set is the only one for which the median scenario produces more energy for all number of stages. The interest of a stochastic method is to account for uncertainty in the future. As we compare our method with the median scenario, if the actual realization of the inflows is close to the median scenario, the stochastic solution will not produce more energy, as the median scenario depicts correctly the future. In practice, this may happen during the fall period, for example when low variability exists in the weather and storms have less chances of developing. This can be seen on Figure 10. Each subfigure

corresponds to a reservoir. The minimum and maximum scenarios are illustrated with the dashed lines. The median scenario is the full line and the actual realization of the inflows is plus sign line. Figure 8a is Chute-du-Diable. The top figure is the day 1 October forecast and the bottom figure is the day 1 September forecast. For the 15 first days, the October forecast median scenario is very close to the inflow realization and therefore, as we keep the day 1 decision only, the median scenario produces more energy. The other subfigures are represented in the same fashion. Again, Figures 10b and 10c show that for Chute-Savane and Lac-St-Jean, the actual inflows in October are very close to the median scenario, therefore there is no gain in using a stochastic optimization model, as the deterministic median scenario allows to obtain a good solution. For this unusual October case, solving the short-term unit commitment and loading problem with a median scenario is acceptable. This affirmation is to be used with caution as situations like these have a low probability of occurring. These results show that there is certainly a gain in using a stochastic model for the short-term hydropower optimization model, as relying on the median scenario offers a less robust solution than multiple scenarios.

6. Conclusion

This paper presents a stochastic short-term hydropower optimization method which emphasizes inflow scenario trees. Few papers looked specifically into stochastic short-term models and we extend the modeling presented in [5] to consider uncertain inflows. The optimization method considers inflow uncertainty, head variations and nonlinear and nonconvex relationship between discharge and power output. The scenario tree generation method first uses kernel density estimation to generate random values of inflows. Then, the path of nodes, from root to leaf, that minimizes the Wasserstein distance is found in the scenario tree and the corresponding nodes are updated using stochastic approximation. The process is repeated until the termination criterion, which is the convergence of the tree in Wasserstein distance, has been reached. A sta-

bility test has shown that the scenario tree generation method is consistent. A highlight of this method is that it uses all data available at each iteration to improve the values of the scenario tree nodes. The scenario trees are inputs to a two phase optimization process. The first phase, loading problem, allows to find water discharge, volume and number of turbines working in each plant. The second phase, unit commitment, chooses the exact combination of turbines to use, to maximize energy production and penalize unit startups. A major feature of this modeling of the problem is that the water head is not neglected. For this paper, the models are tested on three hydropower plants. A rolling horizon procedure is retained on a 31 day planning horizon. The stochastic solution is compared to the median scenario. Furthermore, fast computation time allows this method to be scaled in order to be applied in full to the Saguenay-Lac-St-Jean hydroelectric system. Future work based on this paper consists on investigating the complexity required in the scenario tree structure. Since a rolling-horizon framework is retained and that only the solution of the first stage is kept, tests with scenario fans instead of scenario trees will be conducted.

Acknowledgments

The authors would like to thank Marco Latraverse, and Rio Tinto, for providing data necessary to this study. This work was supported by NSERC, FRQNT and Rio Tinto. Also, a grant for international mobility, awarded by FRQNT through GERAD allowed the research to be conducted at the Norwegian University of Science and Technology. Fleten acknowledges financial support from the Research Council of Norway through project 243964/E20. Alois Pichler gratefully acknowledges support of the Research Council of Norway through grant 207690/E20. The authors are thankful to two anonymous referees, for providing constructive comments that greatly improved the paper.

References

[1] R. Taktak, C. D'Ambrosio, An overview on mathematical programming approaches for the deterministic unit commitment problem in hydro valleys, Energy Systems (2016) 1–23doi:10.1007/s12667-015-0189-x.

[2] E. C. Finardi, E. L. da Silva, Solving the hydro unit commitment problem via dual decomposition and sequential quadratic programming, IEEE Transactions on Power Systems 21 (2) (2006) 835–844. doi:10.1109/TPWRS.2006.873121.

[3] A. Arce, T. Ohishi, S. Soares, Optimal dispatch of generating units of the itaipu hydroelectric plant, IEEE Transactions on Power Systems 17 (1) (2002) 154–158. doi:10.1109/59.982207.

[4] D. Schwanenberg, F. M. Fan, S. Naumann, J. I. Kuwajima, R. A. Montero, A. Assis dos Reis, Short-term reservoir optimization for flood mitigation under meteorological and hydrological forecast uncertainty, Water Resources Management 29 (5) (2015) 1635–1651. doi:10.1007/s11269-014-0899-1.

[5] S. Séguin, P. Côté, C. Audet, Self-scheduling short-term unit commitment and loading problem, IEEE Transactions on Power Systems 31 (1) (2016) 133–142. doi:10.1109/TPWRS.2014.2383911.

[6] S.-E. Fleten, T. K. Kristoffersen, Short-term hydropower production planning by stochastic programming, Computers and Operations Research 35 (8) (2008) 2656 – 2671. doi:10.1016/j.cor.2006.12.022.

[7] A. B. Philpott, M. Craddock, H. Waterer, Hydro-electric unit commitment subject to uncertain demand, European Journal of Operational Research 125 (2) (2000) 410–424. doi:10.1016/S0377-2217(99)00172-1.

[8] T. G. Siqueira, M. Zambelli, M. Cicogna, M. Andrade, S. Soares, Stochastic dynamic programming for long term hydrothermal scheduling considering different streamflow models, in: Probabilistic Methods Applied to Power

Systems, 2006. PMAPS 2006. International Conference on, 2006, pp. 1–6. doi:10.1109/PMAPS.2006.360203.

[9] J. A. Tejada-Guibert, S. A. Johnson, J. R. Stedinger, Comparison of two approaches for implementing multireservoir operating policies derived using stochastic dynamic programming, Water Resources Research 29 (12) (1993) 3969–3980. doi:10.1029/93WR02277.

[10] P. Côté, D. Haguma, R. Leconte, S. Krau, Stochastic optimisation of Hydro-Quebec hydropower installations: a statistical comparison between SDP and SSDP methods, Canadian Journal of Civil Engineering 38 (12) (2011) 1427–1434. doi:10.1139/l11-101.

[11] A. Shapiro, Analysis of stochastic dual dynamic programming method, European Journal of Operational Research 209 (1) (2011) 63 – 72. doi:http://dx.doi.org/10.1016/j.ejor.2010.08.007.

[12] T. Lohmann, A. S. Hering, S. Rebennack, Spatio-temporal hydro forecasting of multireservoir inflows for hydro-thermal scheduling, European Journal of Operational Research 255 (1) (2016) 243 – 258. doi:http://dx.doi.org/10.1016/j.ejor.2016.05.011.

[13] J. R. Birge, F. Louveaux, Introduction to stochastic programming, Springer, 2011. doi:10.1007/978-1-4614-0237-4.

[14] M. Kaut, S. W. Wallace, Evaluation of scenario-generation methods for stochastic programming, no. 14 in Stochastic Programming E-Print Series, Institut für Mathematik, 2003.

[15] D. De Ladurantaye, M. Gendreau, J.-Y. Potvin, Optimizing profits from hydroelectricity production, Computers and Operations Research 36 (2) (2009) 499 – 529. doi:10.1016/j.cor.2007.10.012.

[16] K. Høyland, S. W. Wallace, Generating scenario trees for multistage decision problems, Management Science 47 (2) (2001) 295–307. doi:10.1287/mnsc.47.2.295.9834.

[17] J. Dupačová, G. Consigli, S. W. Wallace, Scenarios for multistage stochastic programs, Annals of Operations Research 100 (1-4) (2000) 25–53. doi:10.1023/A:1019206915174.

[18] Y. Feng, S. M. Ryan, Scenario reduction for stochastic unit commitment with wind penetration, in: PES General Meeting — Conference Exposition, IEEE, 2014, pp. 1–5. doi:10.1109/PESGM.2014.6939138.

[19] N. Growe-Kuska, H. Heitsch, W. Romisch, Scenario reduction and scenario tree construction for power management problems, in: Power Tech Conference Proceedings, 2003 IEEE Bologna, Vol. 3, 2003, p. 7 pp. Vol.3. doi:10.1109/PTC.2003.1304379.

[20] B. Xu, P.-A. Zhong, R. C. Zambon, Y. Zhao, W. W.-G. Yeh, Scenario tree reduction in stochastic programming with recourse for hydropower operations, Water Resources Research 51 (8) (2015) 6359–6380.

[21] F. Babonneau, J.-P. Vial, R. Apparigliato, Uncertainty and Environmental Decision Making: A Handbook of Research and Best Practice, Springer US, Boston, MA, 2010, Ch. Robust Optimization for Environmental and Energy Planning, pp. 79–126. doi:10.1007/978-1-4419-1129-2_3.

[22] W. van Ackooij, R. Henrion, A. Möller, R. Zorgati, Joint chance constrained programming for hydro reservoir management, Optimization and Engineering 15 (2) (2013) 509–531. doi:10.1007/s11081-013-9236-4.

[23] R. Apparigliato, Règles de décision pour la gestion du risque: Application à la gestion hebdomadaire de la production électrique., Ph.D. thesis, Ecole Polytechnique X (2008).

[24] G. Ch. Pflug, A. Pichler, Dynamic generation of scenario trees, Computational Optimization and Applications 62 (3) (2015) 641–668.

[25] T. K. Boomsma, N. Juul, S.-E. Fleten, Bidding in sequential electricity markets: The nordic case, European Journal of Operational Research 238 (3) (2014) 797–809.

[26] Environment Canada prevision models, http://collaboration.cmc.ec.gc.ca/cmc/CMOI/product_guide/docs/changes_f.html, Accessed: 2015-08-21.

[27] C. Brisson, M.-A. Boucher, M. Latraverse, Illustration of the added value of using a multi-site calibration and correction approach to reconstruct natural inflows and inter-catchment transfer flow: a case study, Canadian Journal of Civil Engineering 42 (5) (2015) 342–352. doi:10.1139/cjce-2014-0270.

[28] G. Ch. Pflug, A. Pichler, Convergence of the smoothed empirical process in nested distance, Stochastic Programming E-Print Series, Humboldt University Berlin, 2015.

[29] S. Lloyd, Least squares quantization in PCM, IEEE Transactions on Information Theory 28 (1982) 129–137.

[30] M. C. Jones, The performance of kernel density functions in kernel distribution function estimation, Statistics & Probability Letters 9 (2) (1990) 129 – 132. doi:http://dx.doi.org/10.1016/0167-7152(92)90006-Q.

[31] B. W. Silverman, Density Estimation for Statistics and Data Analysis, Chapman & Hall/CRC Monographs on Statistics & Applied Probability, Taylor & Francis, 1986.

[32] P. Côté, R. Leconte, Comparison of stochastic optimization algorithms for hydropower reservoir operation with ensemble streamflow prediction, Journal of Water Resources Planning and Management 142 (2) (2015) 04015046.

[33] E. K. Aasgård, G. S. Andersen, S.-E. Fleten, D. Haugstvedt, Evaluating a stochastic-programming-based bidding model for a multireservoir system, IEEE Transactions on Power Systems 29 (4) (2014) 1748–1757. doi:10.1109/TPWRS.2014.2298311.

[34] MATLAB, version 8.5.0.197613 (R2015a), The MathWorks Inc., Natick, Massachusetts, 2015.

[35] R. Fourer, D. M. Gay, B. W. Kernighan, AMPL: A Modeling Language for Mathematical Programming, 2nd Edition, Thomson/Brooks/Cole, Pacific Grove, California, 2003.

[36] A. Wächter, L. T. Biegler, On the implementation of an interior-point filter line-search algorithm for large-scale nonlinear programming, Mathematical Programming 106 (1) (2006) 25–57. doi:10.1007/s10107-004-0559-y.

[37] XPRESS Optimization Suite, Fair Isaac Corporation (FICO), www.fico.com/en/products/fico-xpress-optimization-suite/.

[38] A. J. King, S. W. Wallace, Scenario-tree generation: With Michal Kaut, in: Modeling with Stochastic Programming, Springer Series in Operations Research and Financial Engineering, Springer New York, 2012, pp. 77–102. doi:10.1007/978-0-387-87817-1_4.

Appendix A. Notation

The following notation is used throughout the paper:

$i \in \{0, 1, \ldots, N\}$	index of the nodes
$e \in \{1, 2, \ldots, E\}$	index of leaf nodes
$c \in \{1, 2, \ldots, C\}$	index of hydroelectric plants
$r \in \{1, 2, \ldots, u^c\}$	index of hydroelectric plants upstream of plant c
$j \in \{1, 2, \ldots, J\}$	index of scenarios
$s \in \{1, 2, \ldots, n_i^c\}$	index of surfaces corresponding to number of active turbines associated to hydroelectric plant c and node i
$l \in \{1, 2, \ldots, n_i^c\}$	index of combinations associated to hydroelectric plant c and node i
$t \in \{1, 2, \ldots, T^c\}$	index of turbines of hydroelectric plant c
π_j^c	probability of scenario j for plant c
v_i^c	volume of plant reservoir c at node i (hm^3)

q_i^c water discharge at plant c and node i (m^3/s)

θ start-up penalty for any turbine (MW)

β_{li}^c power generated by combination $l \in n_i^c$ at plant c and node i

$$y_{si}^c = \begin{cases} 1 \text{ if surface } s \text{ is chosen at node } i \\ \quad \text{for plant } c \\ 0 \text{ otherwise} \end{cases}$$

$$f_{lit}^c = \begin{cases} 1 \text{ if turbine } t \text{ of combination } l \\ \quad \text{for plant } c \text{ is working at node } i \\ 0 \text{ otherwise} \end{cases}$$

$$x_{li}^c = \begin{cases} 1 \text{ if combination } l \text{ of plant } c \\ \quad \text{is chosen at node } i \\ 0 \text{ otherwise} \end{cases}$$

$$d_{ti}^c = \begin{cases} 1 \text{ if turbine } t \text{ of plant } c \text{ is started} \\ \quad \text{at node } i \\ 0 \text{ otherwise} \end{cases}$$

χ_{si}^c power for surface s at node i and plant c (MW)

$\Psi_s^{Ac}(q_i^c, v_i^c)$ power production function without spillage for surface s and plant c

$\Psi_s^{Bc}(q_i^c, v_i^c)$ power production function with spillage for surface s and plant c

δ_i^c inflow of plant c at node i (m^3/s)

w_i duration of node i (h)

V_j^c final volume for plant c and scenario j

P_j^c expected value of energy produced by scenario j and plant c (loading problem)

E_j^c expected value of energy produced by scenario j and plant c (unit commitment problem)

G_j^c expected value of startups, in energy units, produced by scenario j and plant c

γ conversion factor from water discharge (m^3/s) to (hm^3/h)

$\Phi_j^c(V_j^c)$ water-value function for plant c and scenario j

ζ_i conversion factor to energy units (GWh)

v_{min}^c minimal volume of plant c reservoir (hm^3)

v_{max}^c maximum volume of plant c reservoir (hm^3)

q^c_{min}	minimum water discharge at plant c (m^3/s)
q^c_{max}	maximum water discharge at plant c (m^3/s).